Comparison of 6-^{18}F-Fluorodopamine PET with ^{123}I-Metaiodobenzylguanidine and ^{111}In-Pentetreotide Scintigraphy in Localization of Nonmetastatic and Metastatic Pheochromocytoma

Ioannis Ilias[1], Clara C. Chen[2], Jorge A. Carrasquillo[2], Millie Whatley[2], Alexander Ling[3], Ivica Lazúrová[4], Karen T. Adams[1], Shiromi Perera[1], and Karel Pacak[1]

[1]Reproductive Biology and Adult Endocrinology Program, National Institute of Child Health and Human Development, National Institutes of Health, Bethesda, Maryland; [2]Nuclear Medicine Department, Clinical Center, National Institutes of Health, Bethesda, Maryland; [3]Department of Radiology, Clinical Center, National Institutes of Health, Bethesda, Maryland; and [4]Department of Medicine, Faculty of Medicine, P.J. Šafárik University, Košice, Slovak Republic

We compared functional imaging modalities including PET with 6-^{18}F-fluorodopamine (^{18}F-DA) with ^{123}I-metaiodobenzylguanidine (^{123}I-MIBG) and somatostatin receptor scintigraphy (SRS) with ^{111}In-pentetreotide in nonmetastatic and metastatic pheochromocytoma (PHEO). **Methods:** We studied 25 men and 28 women (mean age ± SD, 44.2 ± 14.2 y) with biochemically proven nonmetastatic (n = 17) or metastatic (n = 36) PHEO. Evaluation included anatomic imaging with CT or MRI and functional imaging that included at least 2 nuclear medicine modalities: ^{18}F-DA PET, ^{123}I-MIBG scintigraphy, or SRS. Sensitivity of functional imaging versus anatomic imaging was assessed on a per-patient and a per-region basis. **Results:** For this available cohort, on a per-patient basis overall sensitivity (combined for nonmetastatic and metastatic PHEO) was 90.2% for ^{18}F-DA PET, 76.0% for ^{123}I-MIBG scintigraphy, and 22.0% for SRS. On a per-region basis, overall sensitivity was 75.4% for ^{18}F-DA PET, 63.4% for ^{123}I-MIBG scintigraphy, and 64.0% for SRS. **Conclusion:** If available, ^{18}F-DA PET should be used in the evaluation of PHEO, because it is more sensitive than ^{123}I-MIBG scintigraphy or SRS. If ^{18}F-DA PET is not available, ^{123}I-MIBG scintigraphy (for nonmetastatic or adrenal PHEO) and SRS (for metastatic PHEO) should be the first alternative imaging methods to be used.

Key Words: radionuclide imaging; ^{18}F-fluorodopamine; ^{123}I-metaiodobenzylguanidine; ^{111}In-pentetreotide; pheochromocytoma

J Nucl Med 2008; 49:1613–1619
DOI: 10.2967/jnumed.108.052373

Until recently, the gold standard functional imaging method for pheochromocytoma (PHEO) was scintigraphy with ^{131}I-metaiodobenzylguanidine (^{131}I-MIBG), with sensitivity of 77%–90% and excellent specificity of 95%–100% (*1*). However, it is scintigraphy with another radionuclide, ^{123}I-MIBG, that offers the option of performing SPECT and is reported to have sensitivity of 83%–100% and specificity of 95%–100% for detecting PHEO (*2–4*). Scintigraphic imaging with ^{123}I-MIBG, compared with ^{131}I-MIBG, is advantageous because of its optimal γ-emissions and lack of β-particles that result in a lower absorbed dose (*5*). Availability of ^{123}I-MIBG, compared with ^{131}I-MIBG, is limited, but is expanding rapidly, especially in the United States. At present, large studies comparing various functional imaging modalities with ^{123}I-MIBG scintigraphy in the evaluation of PHEO are lacking.

PET also enables functional imaging of endocrine tumors. Although PET with ^{18}F-FDG has been used with some success for imaging metastatic PHEO, it is nevertheless a nonspecific ligand that shows uptake in various tumors (*6–8*). Other ligands, for example, ^{11}C-hydroxyephedrine and ^{11}C-epinephrine, have also been used successfully for PET imaging of PHEO (*9–12*). ^{18}F-labeled dihydroxyphenylalanine (^{18}F-DOPA) has enabled PET imaging of benign PHEOs and neck neuroendocrine tumors (*13,14*). Recently, we recommended the use of PET with 6-^{18}F-fluorodopamine (^{18}F-DA) for the detection of PHEO (*15–17*). Our studies have suggested that ^{18}F-DA is a better agent than ^{131}I-MIBG for localization of metastatic PHEO (with 100% sensitivity vs. 56% sensitivity, respectively) (*15,16*). This is probably due to the better affinity of ^{18}F-DA than ^{131}I-MIBG for the norepinephrine membrane transport system and the increased resolution of PET, compared with planar γ-camera imaging.

Received Mar. 2, 2008; revision accepted Jun. 25, 2008.
For correspondence or reprints contact: Karel Pacak, Section on Medical Neuroendocrinology, Reproductive Biology and Adult Endocrinology Program, National Institute of Child Health and Human Development, National Institutes of Health, Building 10, CRC, 1 East, Room 1-3140, 10 Center Dr., MSC-1109, Bethesda, MD 20892-1109.
E-mail: karel@mail.nih.gov

From in vitro and in vivo studies, it has been established that somatostatin receptor subtypes 3 and 4 are expressed in PHEO, including adrenal and metastatic disease (*18–21*). Although somatostatin receptor scintigraphy (SRS) with ^{111}In-pentetreotide (Octreoscan; Mallinckrodt Inc.) has only moderate affinity for these subtypes, compared with subtypes 2 and 5, SRS has been used with variable results to detect this tumor (*18,22–25*). SRS reportedly detects neck paragangliomas with 94%–97% sensitivity (*26–28*) and has higher sensitivity for detecting metastatic PHEO than for detecting benign PHEO (*29*). Nevertheless, in a small study of 10 patients with malignant PHEO and 3 patients with malignant paraganglioma that compared SRS with ^{131}I- or ^{123}I-MIBG scintigraphy, 26 lesions were MIBG- and SRS-positive, 15 lesions were MIBG-positive only, and 7 lesions were SRS-positive only (overall sensitivity for ^{131}I- and ^{123}I-MIBG scintigraphy was 85% and 92%, respectively, for SRS) (*18*).

The aim of this study was to compare ^{18}F-DA PET, ^{123}I-MIBG, and SRS in the localization of adrenal, extra-adrenal, and metastatic or multiple PHEOs in a large study from a single institution. We also evaluated which of these radiopharmaceuticals detected the largest number of lesions in patients with metastatic PHEO. Furthermore, we aimed to give physicians new information and recommendations for the use of various functional imaging methods when a nonmetastatic or metastatic PHEO is localized.

MATERIALS AND METHODS

All patients were enrolled in a study of PHEO approved by the National Institute of Child Health and Human Development Institutional Review Board, and written informed consent was obtained from all patients.

Subjects were retrospectively chosen from a larger group of 178 patients originally enrolled in a study of known or suspected PHEO. Specifically, inclusion criteria for this parent protocol included positive biochemistry, suggestive biochemistry with clinical signs or symptoms of catecholamine excess, and a family history of PHEO, with a tumor found on anatomic imaging studies even without clinical signs or symptoms. Exclusion criteria included inability to give informed consent and refusal or inability (e.g., claustrophobia, previous irradiation, or extreme obesity) to undergo examination, including many imaging studies. Children younger than 18 y and pregnant subjects were also excluded.

From this pool of 178 patients, 53 were retrospectively chosen for inclusion in this study on the basis of confirmed positive biochemical evidence of PHEO (using an in-house assay, as previously described (*30,31*)) and availability of certain imaging studies, including anatomic imaging (CT or MRI) and at least 2 of 3 of the following functional modalities: ^{18}F-DA PET, ^{123}I-MIBG scintigraphy, or SRS. The imaging studies had to be contemporaneously performed within 3 mo of each other.

CT scans of the neck, chest, abdomen, and pelvis were performed on a variety of equipment, including LightSpeed Ultra, LightSpeed QX/i, and HiSpeed CT/i scanners (GE Healthcare) and an Mx8000 IDT scanner (Philips). Section thickness was at the discretion of the radiologist and was set up to 3 mm in the neck, 5 mm in the chest and abdomen, and 7.5 mm in the pelvis, except for 2 cases in which scans of the neck were performed with either 3.75- or 5-mm images and another case in which chest, abdomen, and pelvis images were obtained with 10-mm thickness. All sections were contiguous. All studies were performed with a rapid infusion (130 mL injected at 2 mL/s) of nonionic water-soluble contrast agent.

MRI scans of the neck, chest, abdomen, and pelvis were obtained with 1.5-T Signa scanners (GE Healthcare), except for 1 study performed at an outside institution. Phased-array coils were used for neck imaging, and either phased-array torso or quadrature body coils were used elsewhere. T1-weighted gradient-echo and fat-suppressed, fast spin-echo T2-weighted imaging parameters were adjusted to minimize examination time and achieve desired anatomic coverage. Images were obtained in the axial plane, with additional planes when needed. All studies included a gadolinium–diethylenetriaminepentaacetic acid contrast injection, using fat-suppressed T1-weighted gradient-echo imaging in the axial and coronal planes.

For ^{18}F-DA PET, the patients fasted overnight and were asked to avoid caffeine, tobacco, and alcohol for at least 12 h before the scan. ^{18}F-DA (37 MBq [1.0 mCi]) in 10 mL of normal saline was infused intravenously over 3 min. Attenuation-corrected images were obtained starting immediately after injection. ^{18}F-DA PET was performed using an Advance scanner (GE Healthcare) with a 15-cm field of view. The images were acquired in 2-dimensional mode from the base of the skull to the proximal thigh (in some patients in whom lesions were highly suspected in the head or the lower limbs, the PET studies also fully covered these areas). The emission scan lasted 8–15 min at each level. At least 1 transmission scan lasting 3–5 min was obtained at each level for attenuation correction.

For ^{123}I-MIBG, patients were imaged after intravenous administration of ^{123}I-MIBG (370 MBq [10.0 mCi]). Patients were instructed to take 100 mg of a saturated solution of potassium iodide by mouth twice a day for 4 d, starting the night before ^{123}I-MIBG administration. Medications known to interfere with ^{123}I-MIBG uptake were discontinued. Planar and SPECT images were acquired on a dual-head γ-camera (ADAC Laboratories or Siemens Medical Solutions USA) and a triple-head γ-camera (Trionix XLT; Trionix Laboratories), respectively, equipped with low-energy high-resolution collimators. A total of 120 sequential (40 stops per head) 40-s images were obtained. The images were reconstructed with the manufacturer's software using a standard filtered backprojection algorithm. A Butterworth filter was used for reconstruction. Twenty-four hours after injection, whole-body and SPECT scans of the head through the pelvis were performed. SPECT studies were repeated at 48 h as needed.

For SRS, patients were imaged approximately 4 and 24 h after intravenous administration of ^{111}In-pentetreotide (222 MBq [6 mCi]). Whole-body and SPECT scans of the head through the pelvis were acquired on a dual-head γ-camera (ADAC Laboratories or Siemens Medical Solutions USA) and a triple-head γ-camera (Trionix XLT; Trionix Laboratories), respectively, equipped with medium-energy general-purpose collimators. On occasion, 48-h SPECT images were also obtained. A total of 120 sequential 40-s images were obtained. The images were reconstructed with the manufacturer's software using a standard filtered backprojection algorithm. A Hamming filter was used for reconstruction.

The radiologist who interpreted the CT and MRI findings was unaware of the results of ^{18}F-DA PET, ^{123}I-MIBG scintigraphy, and SRS. Moreover, nuclear medicine studies were read independently of each other and of the anatomic studies by 2 physicians. Sites of uptake outside the normal distribution were considered abnormal. ^{123}I-MIBG uptake in the adrenal glands was considered normal if it

was mild, symmetric, and not enlarged. However, any visualized uptake of ^{18}F-DA in the adrenals was considered to be abnormal, on the basis of previous experience with studies in a small number of healthy volunteers who did not show any adrenal ^{18}F-DA uptake. Abnormal foci seen in nuclear medicine studies were graded on a scale of 1–5 (1, not PHEO; 2, probably not PHEO; 3, equivocal; 4, probably PHEO; and 5, definitely PHEO). Only lesions with scores of 4 and 5 were counted as positive findings. Discrepancies in scans from the first individual masked reading were resolved by a joint meeting of both nuclear medicine physicians in a consensus review (with reexamination and discussion of the studies in question).

Comparison of the results of the nuclear medicine modalities was done on a per-patient and a per-region basis. For the former, scans were considered positive if at least 1 lesion with a score of 4 of 5 or 5 of 5 was seen, regardless of the number of foci (scans with no or equivocal uptake were scored as negative). Because histologic proof of metastatic lesions was largely unavailable, findings on CT or MRI were taken as our reference standard (despite shortcomings of these modalities, as described in the "Discussion" section) for sensitivity calculations of imaging studies. Sensitivity by patient was calculated as follows: the number of patients positive on ^{18}F-DA PET, ^{123}I-MIBG scintigraphy, or SRS divided by the number of patients positive on CT/MRI.

Analysis on a per-region basis was performed over the following areas: left adrenal gland, right adrenal gland, liver, abdominal/pelvic compartment (excluding adrenal glands and liver), lungs, mediastinum, neck, and bone (including skull). For sensitivity calculations, studies were considered either positive or negative, regardless of the number of lesions detected in each region. CT or MRI findings were considered to be the reference standard. Sensitivity by region was calculated as follows: the number of regions positive on ^{18}F-DA PET, ^{123}I-MIBG scintigraphy, or SRS divided by the number of regions positive on CT/MRI. Only regions that were actually covered by ^{18}F-DA PET, ^{123}I-MIBG scintigraphy, or SRS and by either CT or MRI were included.

The McNemar test was used to compare sensitivities between different imaging modalities. A 2-sided P value less than 0.05 was considered significant.

RESULTS

Imaging results from 25 men and 28 women (mean age ± SD, 44.2 ± 14.2 y) with biochemically proven nonmetastatic (n = 17, 2 patients with recurrent disease: 10 patients had T1 N0 M0 disease, stage I; 3 patients had T2 N0 M0 disease, stage II; and 4 had T4 N0 M0 disease, stage IV) or metastatic (n = 36, all with stage IV disease: 9 had T1 N0 M1, 10 had T1 N1 M1, 1 had T2 N0 M1, 1 had T2 N1 M1, 5 had T4 N0 M1, and 10 had T4 N1 M1 disease) PHEOs were assessed. All patients were studied with CT (51 scans) or MRI (47 scans). Two patients had MRI scans only. Functional imaging included ^{18}F-DA PET and ^{123}I-MIBG scintigraphy in 16 patients with nonmetastatic and 35 patients with metastatic PHEO and SRS in 7 patients with nonmetastatic and 18 patients with metastatic PHEO. Five patients with nonmetastatic and 15 with metastatic PHEO were studied with all 3 functional imaging modalities.

Anatomic imaging was positive in all patients. Most lesions seen on CT/MRI showed uptake with at least 1 functional imaging modality. In a few patients, because the enormous number of metastatic lesions did not permit direct one-to-one comparisons, comparisons on a per-patient and a per-region basis were made. In patients with nonmetastatic PHEO, negative functional imaging studies were obtained in 2 patients with ^{18}F-DA PET, 2 patients with ^{123}I-MIBG scintigraphy, and 5 patients with SRS. The following provides more detail, because evaluation on a per-lesion basis was feasible only in these patients with nonmetastatic PHEO: 16 lesions positive on CT/MRI were missed by either ^{18}F-DA PET or ^{123}I-MIBG (in 16 patients), whereas 13 lesions positive on CT/MRI were missed by SRS (in 7 patients). In patients with metastatic PHEO, negative functional imaging studies were obtained in 4 patients with ^{18}F-DA PET, 9 patients with ^{123}I-MIBG scintigraphy, and 1 patient with SRS.

For this available cohort, on a per-patient basis, sensitivity was equal for ^{18}F-DA PET and ^{123}I-MIBG scintigraphy (87.5%) and lower for SRS (28.5%) in patients with nonmetastatic PHEO (Table 1). In patients with metastatic PHEO, sensitivity was 91.4% for ^{18}F-DA PET, 70.6% for ^{123}I-MIBG, and 88.9% for SRS (Table 1). Overall sensitivity (combined for nonmetastatic and metastatic PHEO) was 90.2% for ^{18}F-DA PET, 76.0% for ^{123}I-MIBG, and 22.0% for SRS. Furthermore, on a per-region basis, sensitivity was 67% for ^{18}F-DA PET, 75% for ^{123}I-MIBG, and 37.5% for SRS in patients with nonmetastatic PHEO (Table 2). In patients with metastatic PHEO,

TABLE 1
Results and Comparisons of Imaging Modalities by Patient

Patients with...	No. of patients positive on functional imaging	No. of patients positive on CT/MRI	Sensitivity of functional imaging modality (%)
Nonmetastatic PHEO	14 (^{18}F-DA)	16	87.5
	14 (^{123}I-MIBG)	16	87.5
	2 (SRS)	7	28.5*
Metastatic PHEO	32 (^{18}F-DA)	35	91.4
	24 (^{123}I-MIBG)	34	70.6
	16 (SRS)	18	88.9

*P = 0.0625, McNemar test.
Sensitivity of functional imaging studies was calculated on basis of number of CT/MRI studies used as reference standard.

TABLE 2
Results and Comparisons of Imaging Modalities by Region

Patients with...	No. of positive regions with foci of uptake	No. of positive CT/MRI regions	Sensitivity of functional imaging modality (%)
Nonmetastatic PHEO	20 (^{18}F-DA)	30	67.0*
	21 (^{123}I-MIBG)	28	75.0†
	3 (SRS)	8	37.5‡
Metastatic PHEO	69 (^{18}F-DA)	88	78.4*
	56 (^{123}I-MIBG)	95	58.9*
	37 (SRS)	54	68.5*

*P = 0.001, McNemar test.
†P = 0.01, McNemar test.
‡P = 0.0625, McNemar test.
Sensitivity of functional imaging studies was calculated on basis of number of CT/MRI studies used as reference standard. Regions included left adrenal gland, right adrenal gland, liver, abdominal/pelvic compartment (excluding adrenal glands and liver), lungs, mediastinum, neck, and bone (including head or skull).

sensitivity was 78.4% for ^{18}F-DA PET, 58.9% for ^{123}I-MIBG, and 68.5% for SRS (Table 2). Overall sensitivity (combined for nonmetastatic and metastatic PHEO) was 75.4% for ^{18}F-DA PET, 63.4% for ^{123}I-MIBG, and 64.0% for SRS.

In several patients, functional imaging modalities showed lesions in regions that were negative on CT or MRI. With ^{18}F-DA PET, compared with CT or MRI, lesions were shown in 5 more patient regions in 5 patients (in the adrenals or the abdominal or pelvic compartment), and with ^{123}I-MIBG scintigraphy, 1 additional positive region in 1 patient (in the right adrenal) was seen.

In patients with nonmetastatic PHEO who were studied with all 3 functional imaging modalities, ^{18}F-DA PET and ^{123}I-MIBG scintigraphy were more positive on a per-patient and on a per-region basis than was SRS (Table 3; Fig. 1). In patients with metastatic PHEO who were studied with all 3 functional imaging modalities, ^{18}F-DA PET and SRS were more positive on a per-patient basis than was ^{123}I-MIBG scintigraphy, whereas on a per-region basis, SRS was more positive than were ^{18}F-DA PET and ^{123}I-MIBG scintigraphy (Table 3; Fig. 2).

TABLE 3
Results and Comparisons Among Functional Imaging Modalities by Patient and by Region

Patients with...	Functional imaging modality	No. of patients positive	No. of regions positive
Nonmetastatic PHEO (n = 5)	^{18}F-DA	5	6
	^{123}I-MIBG	5	5
	SRS	1	1
Metastatic PHEO (n = 15)	^{18}F-DA	14	31
	^{123}I-MIBG	10	31
	SRS	15	44

Regions included left adrenal gland, right adrenal gland, liver, abdominal/pelvic compartment (excluding adrenal glands and liver), lungs, mediastinum, neck, and bone (including head or skull).

DISCUSSION

In this largest-to-date comparison study of ^{18}F-DA PET with ^{123}I-MIBG scintigraphy and SRS in 17 patients with nonmetastatic PHEO and 36 patients with metastatic PHEO, overall more foci of uptake were shown with ^{18}F-DA PET than with the other functional imaging modalities. In nonmetastatic PHEO, ^{18}F-DA PET imaged slightly fewer foci than did ^{123}I-MIBG scintigraphy (and both detected more foci than did SRS), but in metastatic PHEO, ^{18}F-DA PET detected more foci than did ^{123}I-MIBG scintigraphy and SRS. Some, mainly metastatic, lesions were localized by 1 modality only, but no distinct pattern for any particular tumor size or

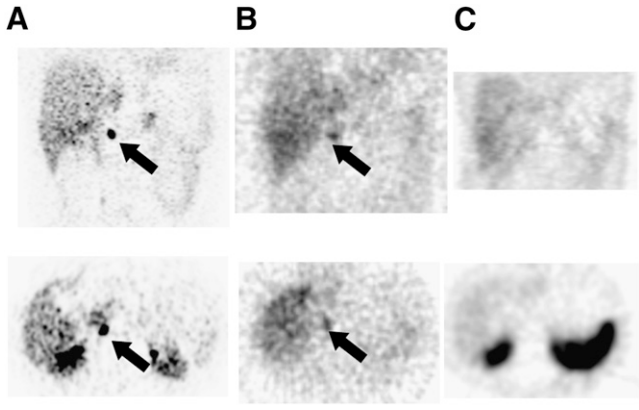

FIGURE 1. Coronal (upper row) and transverse (lower row) ^{18}F-DA (A), 24-h ^{123}I-MIBG (B), and 4-h SRS (C) images of 23-y-old man with nonmetastatic recurrent right adrenal PHEO. ^{18}F-DA PET and ^{123}I-MIBG scintigraphy are both positive (arrows), whereas SRS is negative.

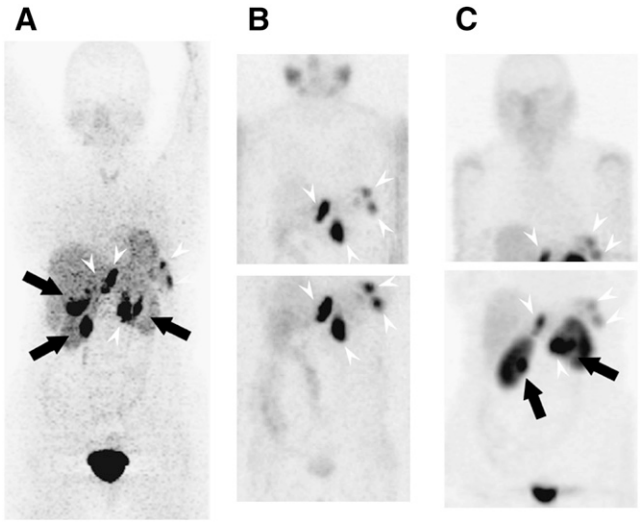

FIGURE 2. Reprojected ^{18}F-DA (A), 24-h ^{123}I-MIBG (B), and 4-h SRS (C) images of 60-y-old woman with left adrenal PHEO and peritoneal and retroperitoneal metastases (arrowheads). ^{18}F-DA PET and SRS (arrows) show more lesions than does ^{123}I-MIBG scintigraphy.

region emerged. Overall, the scintigraphic modality with the highest sensitivity for localizing PHEO was ^{18}F-DA PET (75.4%), followed by ^{123}I-MIBG (63.4%) and SRS (64%).

In many patients with PHEO (especially in those with extraadrenal PHEO, adrenal PHEO larger than 5 cm, or mutations of genes encoding mainly subunits B and D of the mitochondrial enzyme succinate dehydrogenase [SDHB and SDHD]), the possibility of metastatic disease or multiple tumors should be considered (or excluded). For this, functional imaging modalities are most useful (*3,6,9,16,17,32–34*). The sensitivity of CT and MRI for detecting extraadrenal or metastatic PHEO is approximately 90% (or lower, when postoperative changes prevent the correct localization of tumors) (*35–39*). Moreover, the specificities of both CT and MRI scans are disappointingly low (as low as 60%) in localizing PHEO (particularly metastatic PHEO) (*3*). In this study, both CT and MRI also missed lesions that were detected by functional imaging studies. Although we do not have surgical confirmation that the lesions seen on functional imaging and not on anatomic imaging were PHEO, we were confident that most of them were real based on clinical follow-up, including improvement after chemotherapy or ^{131}I-MIBG therapy in many cases.

PET is a physiologic method of imaging that depends on selective binding or uptake and retention of radiolabeled agents by different tissues. It has the advantages of rapid imaging and high spatial and temporal resolution. Several PET agents have been used for localizing PHEO, including ^{18}F-FDG (*6,12,40*), ^{11}C-hydroxyephedrine (*10,12,41*), ^{11}C-epinephrine (*11*), ^{18}F-DA (*15,16*), and ^{18}F-DOPA (*13,14*). A comparison study of ^{131}I- and ^{123}I-MIBG and ^{18}F-FDG PET scans in patients with malignant PHEO showed that ^{18}F-FDG PET was superior to MIBG (*6*). Furthermore, ^{18}F-FDG PET was recently shown to be superior to ^{18}F-DA or ^{123}I-MIBG in localizing metastases of highly malignant paragangliomas (in particular those with SHDB mutations) (*7*). However, ^{18}F-FDG remains nonspecific for PHEO, as ^{18}F-FDG also detects many other types of tumors. PET with ^{11}C-hydroxyephedrine and ^{11}C-epinephrine has yielded better results than has PET with ^{18}F-FDG for the diagnostic localization of PHEO, although the short physical half-lives ($t_{1/2}$ = 20 min) of these radiopharmaceuticals will likely preclude their more widespread use (*10,12,41*). Recently, PET with ^{18}F-DOPA, a labeled precursor of dopamine, was used in a study of 14 patients with benign adrenal PHEO and a small number of patients (n = 3) with extraadrenal nonmetastatic PHEO (*14*). In the former group, all tumors were localized with ^{18}F-DOPA PET, whereas in the latter group, ^{18}F-DOPA PET was concordant with MRI results in 1 of 3 patients and imaged a tumor that was not seen with ^{131}I-MIBG scintigraphy (*14*). In another study of 10 patients with glomus jugulare tumors (which arise from the paraganglionic tissue of the head and neck and are similar to PHEOs), 11 of the 15 presumed tumors diagnosed by ^{18}F-DOPA PET were confirmed by MRI (*13*).

At the National Institutes of Health, we have used ^{18}F-DA with excellent results in localizing both adrenal and extraadrenal PHEOs, including metastatic lesions (*15,16,42,43*). In a previous study of patients with metastatic PHEO, we found that ^{18}F-DA PET was clearly superior to ^{131}I-MIBG (with sensitivities of 100% and 56%, respectively) (*16*). The availability of ^{123}I-MIBG prompted us to compare it with ^{18}F-DA PET as well. In the present study, in patients with nonmetastatic (mainly adrenal) PHEOs, ^{18}F-DA and ^{123}I-MIBG had equivalent sensitivities for tumor detection, and both were superior to SRS. In patients with metastatic disease, ^{18}F-DA was superior to ^{123}I-MIBG and detected more lesions. In a minority of these patients, SRS showed impressively more lesions than did ^{123}I-MIBG. Additional advantages of PET, compared with other functional imaging modalities, include the means of immediate whole-body imaging, the possibility of quantitative assessment of uptake, and the absence of artifacts from scar tissue or from the presence of metallic clips after surgery (*44*). In fact, ^{18}F-DA scan artifacts appear to be quite rare, and in this study no artifacts were noted except for mild adrenal uptake in some patients, which was scored as abnormal (although we have since found that this can be normal). Known artifacts with ^{18}F-DA scans also include uptake in adrenal hyperplasia and metabolically active brown fat.

In PHEO, ^{131}I-MIBG offers high specificity (95%–100%) with lower sensitivity (56%–77%) (*43,45*). Sensitivity is elevated to 78%–91%, and specificity is preserved (*3,46,47*) using ^{123}I-MIBG. In the present study, ^{123}I-MIBG was as sensitive as ^{18}F-DA and definitely superior to SRS in localizing nonmetastatic PHEO. However, in the evaluation of metastatic PHEO, ^{123}I-MIBG was the least informative scintigraphic modality, lagging behind ^{18}F-DA and SRS.

SRS is used effectively for the diagnostic localization of neuroendocrine tumors (*48,49*). In a small number of reports

comparing the diagnostic accuracy of SRS with ^{123}I- or ^{131}I-MIBG in patients with metastatic PHEO, SRS had an overall higher detection rate: SRS found up to 87% of lesions, whereas ^{123}I-MIBG localized only 57% (*4,18,24,25,29*).

SRS studies may be particularly useful as a functional imaging modality in patients with rapidly progressing and growing PHEOs. In these PHEOs, changes in genetic and cellular characteristics occur, currently by unknown mechanisms such as the expression of somatostatin receptors. In this study, SRS failed to detect the 5 of 7 tumors in patients with nonmetastatic disease. However, in metastatic PHEO, although ^{18}F-DA localized many lesions that SRS did not, SRS also showed a substantial number of metastatic lesions that were not detected with ^{18}F-DA. In addition, SRS showed more lesions than did ^{123}I-MIBG in patients with metastatic disease (^{123}I-MIBG provided the least additional information in these patients). Clinically, patients with predominantly SRS-positive lesions had rapidly progressing tumors on the basis of our clinical follow-up, repeated biochemistry, and anatomic imaging studies.

This report has shortcomings that should be mentioned. First, only 1 patient with extraadrenal nonmetastatic PHEO was studied, and future studies are needed to address this subset of patients. Second, only 5 patients with nonmetastatic PHEO were studied with all 3 functional imaging modalities, a deficiency that needs to be addressed as well. Third, most patients with metastatic PHEO did not undergo surgery, as it could not be justified clinically, and therefore, surgical confirmation of disease is not available for most lesions in these patients. Fourth, fewer SRS studies than ^{18}F-DA and ^{123}I-MIBG studies were performed; with such unequal size groups, selection bias toward performing SRS studies in patients with metastatic disease may have occurred. Fifth, we considered ^{18}F-DA uptake in the adrenals as being abnormal. However, with further experience and the use of PET/CT, we have since found that healthy adrenal glands in some patients may demonstrate mild adrenal uptake of ^{18}F-DA (lean body mass, maximum standardized uptake value < 7.3) (*50*). Finally, ascertainment bias (i.e., the tendency to produce false results and conclusions based on a distorted or nontypical sample) may have occurred, principally due to the rareness of the tumors that were studied. Nevertheless, despite negative MIBG scans before referral in 1 patient with nonmetastatic and 4 with metastatic PHEOs, all the study subjects had biochemical proof of disease.

CONCLUSION

In the diagnostic evaluation of PHEO, ^{18}F-DA PET and ^{123}I-MIBG are more sensitive than SRS in detecting nonmetastatic primary adrenal PHEO. For metastatic PHEO, ^{18}F-DA is more sensitive than SRS, and both are superior to ^{123}I-MIBG. In patients with rapidly progressing and growing PHEOs, SRS may detect lesions that are negative on both ^{18}F-DA and ^{123}I-MIBG scans. In a study of patients with familial-SDHB–associated disease, PET with ^{18}F-FDG was shown to be the superior functional imaging method. In those patients with PHEO in whom anatomic imaging modalities indicate adrenal disease, ^{123}I-MIBG is a valuable imaging modality to be used; this modality is comparable with other specific imaging methods such as ^{18}F-DA PET. For those with metastatic disease, SRS can be used. However, this approach should not exclude ^{18}F-DA PET, which is as sensitive as ^{123}I-MIBG and SRS for detecting nonmetastatic and metastatic PHEO, respectively. As PET becomes more available, either ^{18}F-DA PET or PET with another specific PET ligand will become the method of choice for functional imaging of nonmetastatic and metastatic PHEO.

ACKNOWLEDGMENTS

This work was supported in part by the Intramural Research Program of the National Institute of Child Health and Human Development.

REFERENCES

1. Sisson JC, Shulkin BL. Nuclear medicine imaging of pheochromocytoma and neuroblastoma. *Q J Nucl Med.* 1999;43:217–223.
2. Nielsen JT, Nielsen BV, Rehling M. Location of adrenal medullary pheochromocytoma by I-123-metaiodobenzylguanidine SPECT. *Clin Nucl Med.* 1996;21:695–699.
3. Furuta N, Kiyota H, Yoshigoe F, Hasegawa N, Ohishi Y. Diagnosis of pheochromocytoma using [^{123}I]- compared with [^{131}I]-metaiodobenzylguanidine scintigraphy. *Int J Urol.* 1999;6:119–124.
4. van der Harst E, de Herder WW, Bruining HA, et al. [^{123}I]metaiodobenzylguanidine and [^{111}In]octreotide uptake in benign and malignant pheochromocytomas. *J Clin Endocrinol Metab.* 2001;86:685–693.
5. International Commission on Radiological Protection. *Radiation Dose to Patients from Radiopharmaceuticals.* ICRP Publication 53. Oxford, U.K.: Pergamon Press; 1988:329–331.
6. Shulkin BL, Thompson NW, Shapiro B, Francis IR, Sisson JC. Pheochromocytomas: imaging with 2-[fluorine-18]fluoro-2-deoxy-D-glucose PET. *Radiology.* 1999;212:35–41.
7. Timmers HJ, Kozupa A, Chen CC, et al. Superiority of fluorodeoxyglucose positron emission tomography to other functional imaging techniques in the evaluation of metastatic SDHB-associated pheochromocytoma and paraganglioma. *J Clin Oncol.* 2007;25:2262–2269.
8. Mamede M, Carrasquillo JA, Chen CC, et al. Discordant localization of 2-[^{18}F]-fluoro-2-deoxy-D-glucose in 6-[^{18}F]-fluorodopamine- and [^{123}I]-metaiodobenzylguanidine-negative metastatic pheochromocytoma sites. *Nucl Med Commun.* 2006;27:31–36.
9. Trampal C, Engler H, Juhlin C, Bergstrom M, Langstrom B. Pheochromocytomas: detection with ^{11}C hydroxyephedrine PET. *Radiology.* 2004;230:423–428.
10. Shulkin BL, Wieland DM, Schwaiger M, et al. PET scanning with hydroxyephedrine: an approach to the localization of pheochromocytoma. *J Nucl Med.* 1992;33:1125–1131.
11. Shulkin BL, Wienland DM, Shapiro B, Sisson JC. PET epinephrine studies of pheochromocytoma [abstract]. *J Nucl Med.* 1995;36(suppl):229P.
12. Mann GN, Link JM, Pham P, et al. [^{11}C]metahydroxyephedrine and [^{18}F]fluorodeoxyglucose positron emission tomography improve clinical decision making in suspected pheochromocytoma. *Ann Surg Oncol.* 2006;13:187–197.
13. Hoegerle S, Ghanem N, Altehoefer C, et al. ^{18}F-DOPA positron emission tomography for the detection of glomus tumours. *Eur J Nucl Med Mol Imaging.* 2003;30:689–694.
14. Hoegerle S, Nitzsche E, Altehoefer C, et al. Pheochromocytomas: detection with ^{18}F DOPA whole-body PET—initial results. *Radiology.* 2002;222:507–512.
15. Pacak K, Eisenhofer G, Carrasquillo JA, Chen CC, Li ST, Goldstein DS. 6-[^{18}F]fluorodopamine positron emission tomographic (PET) scanning for diagnostic localization of pheochromocytoma. *Hypertension.* 2001;38:6–8.
16. Ilias I, Yu J, Carrasquillo J, et al. Superiority of 6-[^{18}F]-fluorodopamine positron emission tomography versus [^{131}I]-metaiodobenzylguanidine scintigraphy in the

localization of metastatic pheochromocytoma. *J Clin Endocrinol Metab.* 2003; 88:4083–4087.
17. Ilias I, Pacak K. Current approaches and recommended algorithm for the diagnostic localization of pheochromocytoma. *J Clin Endocrinol Metab.* 2004; 89:479–491.
18. Tenenbaum F, Lumbroso J, Schlumberger M, et al. Comparison of radiolabeled octreotide and meta-iodobenzylguanidine (MIBG) scintigraphy in malignant pheochromocytoma. *J Nucl Med.* 1995;36:1–6.
19. Mundschenk J, Lehnert H. Malignant pheochromocytoma. *Exp Clin Endocrinol Diabetes.* 1998;106:373–376.
20. Ueberberg B, Tourne H, Redman A, et al. Differential expression of the human somatostatin receptor subtypes sst1 to sst5 in various adrenal tumors and normal adrenal gland. *Horm Metab Res.* 2005;37:722–728.
21. Unger N, Serdiuk I, Sheu SY, et al. Immunohistochemical determination of somatostatin receptor subtypes 1, 2A, 3, 4, and 5 in various adrenal tumors. *Endocr Res.* 2004;30:931–934.
22. Krenning EP, Kwekkekeboom DJ, Bakker WH, et al. Somatostatin receptor scintigraphy with [^{111}In-DTPA-D-phe1]- and [^{123}I-Tyr3]-octreotide: the Rotterdam experience with more than 1000 patients. *Eur J Nucl Med.* 1993;20: 716–731.
23. Lauriero F, Rubini G, D'Addabo F, Rubini D, Schettini F, D'Addabo A. I-131 MIBG scintigraphy of neuroectodermal tumors: comparison between I-131 MIBG and In-DTPA-octreotide. *Clin Nucl Med.* 1995;20:243–249.
24. Limouris GS, Giannakopoulos V, Stavraka A, Toubanakis N, Vlahos L. Comparison of In-111 pentetreotide, Tc-99m (V)DMSA and I-123 MIBG scintimaging in neural crest tumors. *Anticancer Res.* 1997;17:1589–1592.
25. Lastoria S, Maurea S, Vergara E, et al. Comparison of labeled MIBG and somatostatin analogs in imaging neuroendocrine tumors. *Q J Nucl Med.* 1995; 39:145–149.
26. Bustillo A, Telischi F, Weed D, et al. Octreotide scintigraphy in the head and neck. *Laryngoscope.* 2004;114:434–440.
27. Duet M, Sauvaget E, Petelle B, et al. Clinical impact of somatostatin receptor scintigraphy in the management of paragangliomas of the head and neck. *J Nucl Med.* 2003;44:1767–1774.
28. Whiteman ML, Serafini AN, Telischi FF, Civantos FJ, Falcone S. ^{111}In octreotide scintigraphy in the evaluation of head and neck lesions. *AJNR.* 1997;18: 1073–1080.
29. Kaltsas G, Korbonits M, Heintz E, et al. Comparison of somatostatin analog and meta-iodobenzylguanidine radionuclides in the diagnosis and localization of advanced neuroendocrine tumors. *J Clin Endocrinol Metab.* 2001;86:895–902.
30. Eisenhofer G, Lenders JW, Linehan WM, Walther MM, Goldstein DS, Keiser HR. Plasma normetanephrine and metanephrine for detecting pheochromocytoma in von Hippel-Lindau disease and multiple endocrine neoplasia type 2. *N Engl J Med.* 1999;340:1872–1879.
31. Lenders JW, Keiser HR, Goldstein DS, et al. Plasma metanephrines in the diagnosis of pheochromocytoma. *Ann Intern Med.* 1995;123:101–109.
32. Pacak K, Eisenhofer G, Goldstein DS. Functional imaging of endocrine tumors: role of positron emission tomography. *Endocr Rev.* 2004;25:568–580.
33. Ezuddin S, Fragkaki C. MIBG and FDG PET findings in a patient with malignant pheochromocytoma: a significant discrepancy. *Clin Nucl Med.* 2005;30:579–581.
34. Shirkare S, Kuwert T, Weckesser M, Czech N, Langen KJ, Muller-Gartner HW. Localization of a pheochromocytoma using I-123 MIBG adrenal scintigraphy. *J Postgrad Med.* 1994;40:85–87.
35. Bravo EL. Evolving concepts in the pathophysiology, diagnosis and treatment of pheochromocytoma. *Endocr Rev.* 1994;15:356–358.
36. Mannelli M, Ianni L, Cilotti A, Conti A. Pheochromocytoma in Italy: a multicentric retrospective study. *Eur J Endocrinol.* 1999;142:619–624.
37. Maurea S, Cuocolo A, Reynolds JC, Neumann RD, Salvatore M. Diagnostic imaging in patients with paragangliomas: computed tomography, magnetic resonance and MIBG scintigraphy comparison. *Q J Nucl Med.* 1996;40:365–371.
38. Shapiro B, Sisson JC, Shulkin BL, Gross MD, Zempel S. The current status of meta-iodobenzylguanidine and related agents for the diagnosis of neuroendocrine tumors. *Q J Nucl Med.* 1995;39(4, suppl 1):S3–S8.
39. Schmedtje JFJ, Sax S, Pool JL, Goldfarb RA, Nelson EB. Localization of ectopic pheochromocytomas by magnetic resonance imaging. *Am J Med.* 1987;83: 770–772.
40. Taniguchi K, Ishizu K, Torizuka T, et al. Metastases of predominantly dopamine-secreting phaeochromocytoma that did not accumulate meta-iodobenzylguanidine: imaging with whole body positron emission tomography using ^{18}F-labelled deoxyglucose. *Eur J Surg.* 2001;167:866–870.
41. Trampal C, Hengler H, Juhlin C, Bergstrom M, Langstrom B. Detection of pheochromocytoma using ^{11}C-hydroxyephedrine-PET [abstract]. *Radiology.* 2002;225(suppl):S425.
42. Pacak K, Linehan WM, Eisenhofer G, Walther MM, Goldstein DS. Recent advances in genetics, diagnosis, localization and treatment of pheochromocytoma. *Ann Intern Med.* 2001;134:315–329.
43. Pacak K, Goldstein DS, Doppman JL, Shulkin BL, Udelsman R, Eisenhofer G. A "pheo" lurks: novel approaches for locating occult pheochromocytoma. *J Clin Endocrinol Metab.* 2001;86:3641–3646.
44. Brink I, Hoegerle S, Klisch J, Bley TA. Imaging of pheochromocytoma and paraganglioma. *Fam Cancer.* 2005;4:61–68.
45. Fujita A, Hyodoh H, Kawamura Y, Kanegae K, Furuse M, Kanazawa K. Use of fusion images of I-131 metaiodobenzylguanidine, SPECT and magnetic resonance studies to identify a malignant pheochromocytoma. *Clin Nucl Med.* 2000;25:440–442.
46. Lumachi F, Tregnaghi A, Zucchetta P, et al. Sensitivity and positive predictive value of CT, MRI and ^{123}I-MIBG scintigraphy in localizing pheochromocytomas: a prospective study. *Nucl Med Commun.* 2006;27:583–587.
47. Cecchin D, Lumachi F, Marzola MC, et al. A meta-iodobenzylguanidine scintigraphic scoring system increases accuracy in the diagnostic management of pheochromocytoma. *Endocr Relat Cancer.* 2006;13:525–533.
48. van der Lely AJ, de Herder WW, Krenning EP, Kwekkeboom DJ. Octreoscan radioreceptor imaging. *Endocrine.* 2003;20:307–311.
49. Breeman WA, De Jong M, Kwekkeboom DJ, et al. Somatostatin receptor-mediated imaging and therapy: basic science, current knowledge, limitations and future perspectives. *Eur J Nucl Med.* 2001;28:1412–1429.
50. Timmers HJ, Carrasquillo JA, Whatley M, et al. Usefulness of standardized uptake values for distinguishing adrenal glands with pheochromocytoma from normal adrenal glands by use of 6-^{18}F-fluorodopamine PET. *J Nucl Med.* 2007;48: 1940–1944.